Supporting information

Glycerol-assisted Grain Modulation in Femtosecond-Laser-induced Photochemical Synthesis of Patterned ZnO Nanomaterials

Yingchen Wang,† # *Songyan Xue,*† # *Yinuo Xu,*† *Jing Long,*† *Binzhang Jiao,*† *Hui Gao,*† *Xuhao Fan,*† *Yuncheng Liu,*† *Leimin Deng,*† ‡ *and Wei Xiong*† ‡ *.

† *Wuhan National Laboratory for Optoelectronics, School of Optical and Electronic Information, Huazhong University of Science and Technology, Wuhan 430074, China.*

‡ *Optics Valley Laboratory, Hubei 430074, China*

# These authors contributed equally.

*E-mail: weixiong@hust.edu.cn

Contents:

Supporting Figures:

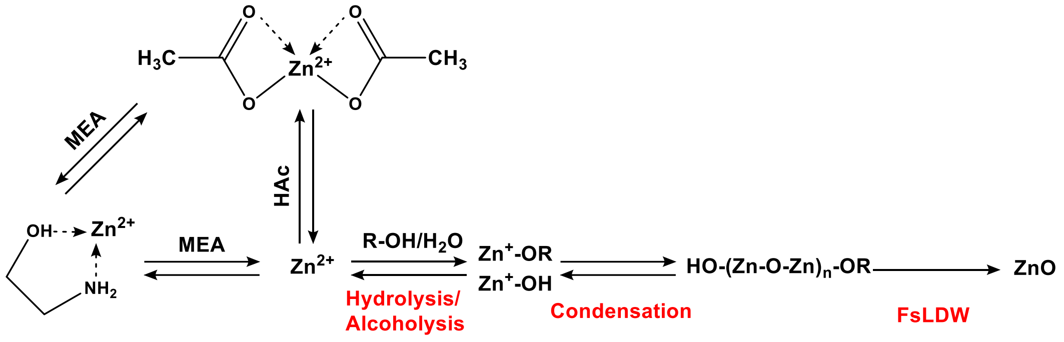

Figure S1. Chemical reactions of components during the precursor preparation and FsLDW.

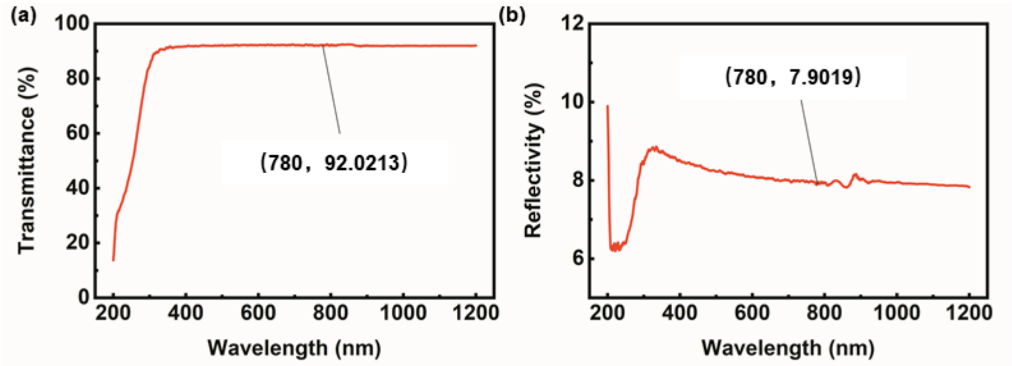

Figure S2. Transmittance (a) and reflectance (b) of the soda-lime glass substrate.

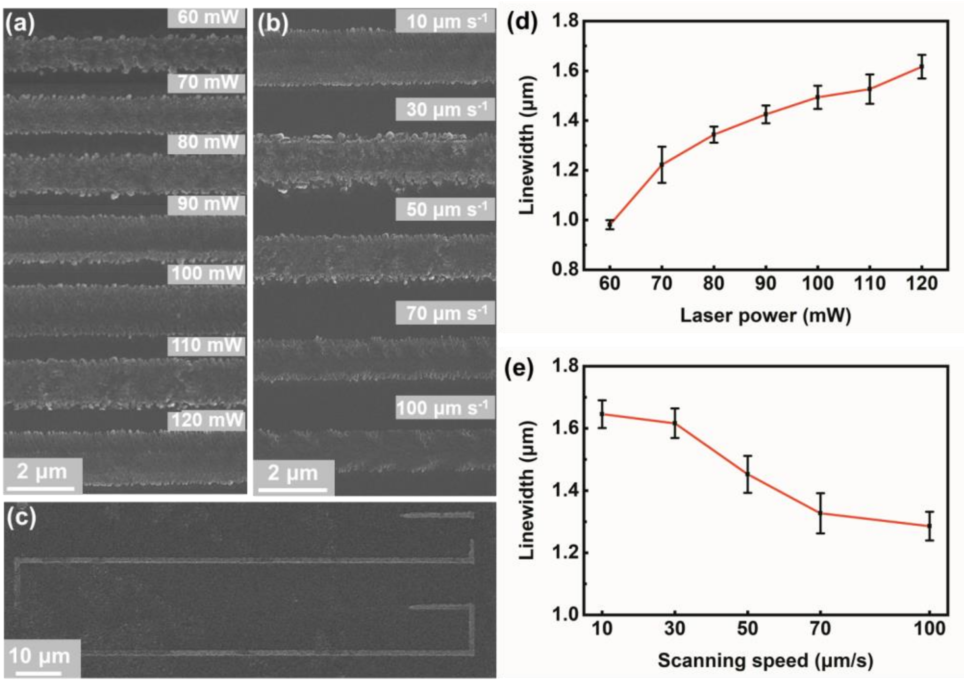

Figure S3. SEM images of ZnO microstructures fabricated with different laser power

(a) (d) ranging from 60 mW to 120 mW when the scanning speed is 10 μm s^{-1} and scanning speeds (b) (e) ranging from 10 μm s^{-1} to 100 μm s^{-1} when laser power is 120 mW; (c) SEM images of ZnO microstructures fabricated with laser power of 120 mW and scanning speed of 120 μm s^{-1}.

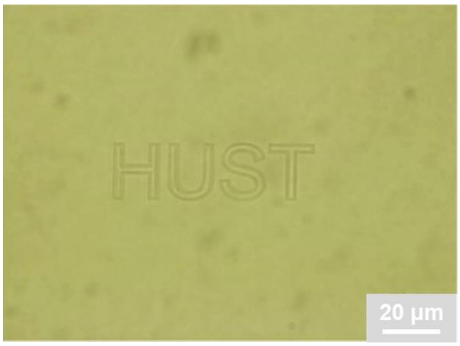

Figure S4. The optical image of the FLDW results on the flexible substrate (PI).

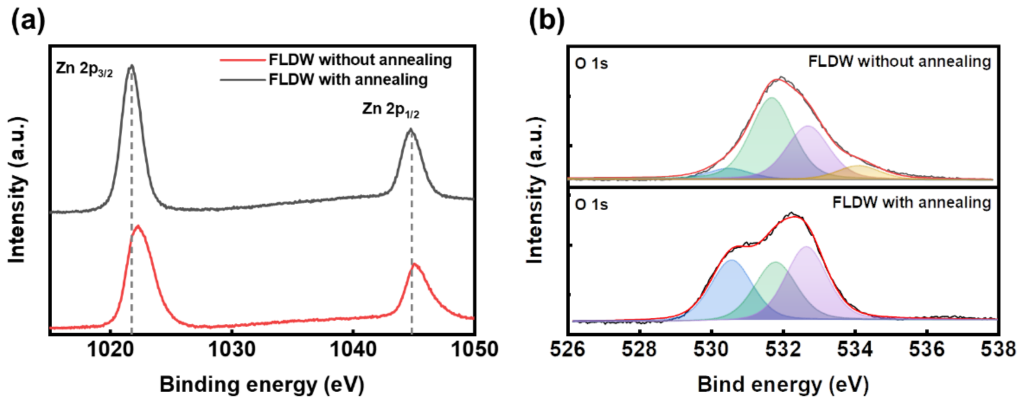

Figure S5. XPS spectra of the (a) Zn 2p and (b) O 1s of ZnO fabricated by femtosecond laser direct writing with and without thermal annealing, respectively.

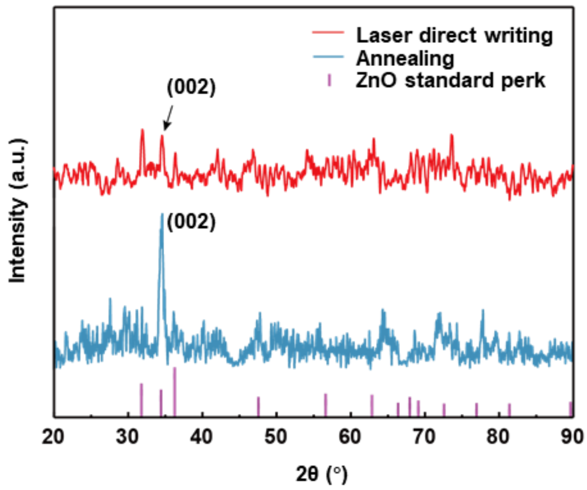

Figure S6. XRD curves of laser-fabricated zinc oxide synthesized by FLDW and annealing at 550°C for 2 hours correspond to the indexation of the diffraction peaks for zinc oxide.

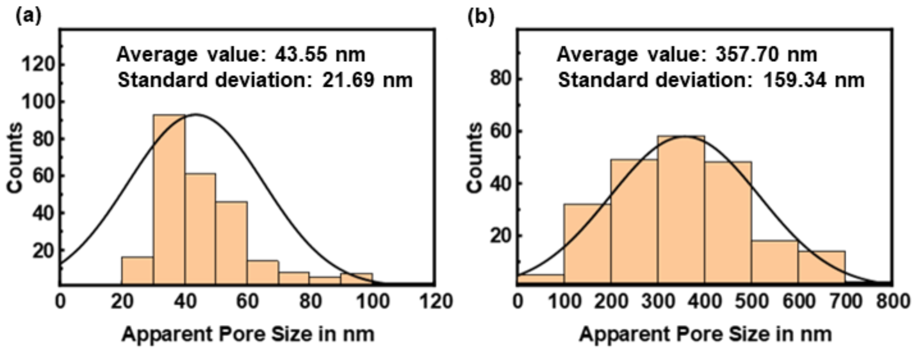

Figure S7. Grain size distribution of the FsLDW products with 20 vol.% glycerol (a) and without (b).

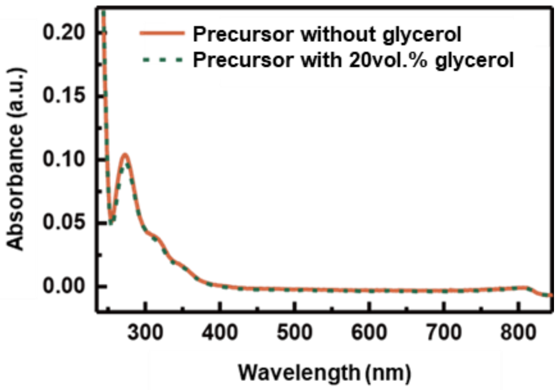

Figure S8. The absorption spectrum of the precursor solution with or without glycerol.

M_r	Molecular formula	M_r	Molecular formula
155	$Zn(OH)_2$	309	$(CH_3COO)Zn^+$ $Zn^+(CH_3COO)$
184	$Zn(CH_3COO)_2$	341	$(CH_3COO)Zn^+$ $Zn^+(CH_3COO)$ OH HO
199	$Zn(CH_3COO)(OH)$	369	$(CH_3COO)Zn^+$ $Zn^+(CH_3COO)$
215	$(C_3H_8O_2)\cdots\rightarrow Zn^{2+}\leftarrow\cdots(C_3H_8O_2)$	383	(CH_3COO)—Zn—O—Zn—(CH_3COO)
241	$Zn(CH_3COO)_2$	397	$(C_3H_8O_2)\cdots\rightarrow Zn^{2+}$ $Zn^{2+}\leftarrow\cdots(C_3H_8O_2)$
Notes	= H_2C—NH_2, H_2C—OH		$(C_3H_8O_2)\cdots\rightarrow$ = H_3C—O—CH_2—CH_2—OH$\cdots\rightarrow$

Figure S9. Substances contained in the analysis results of liquid chromatography–mass spectrometry and their relative molecular masses.

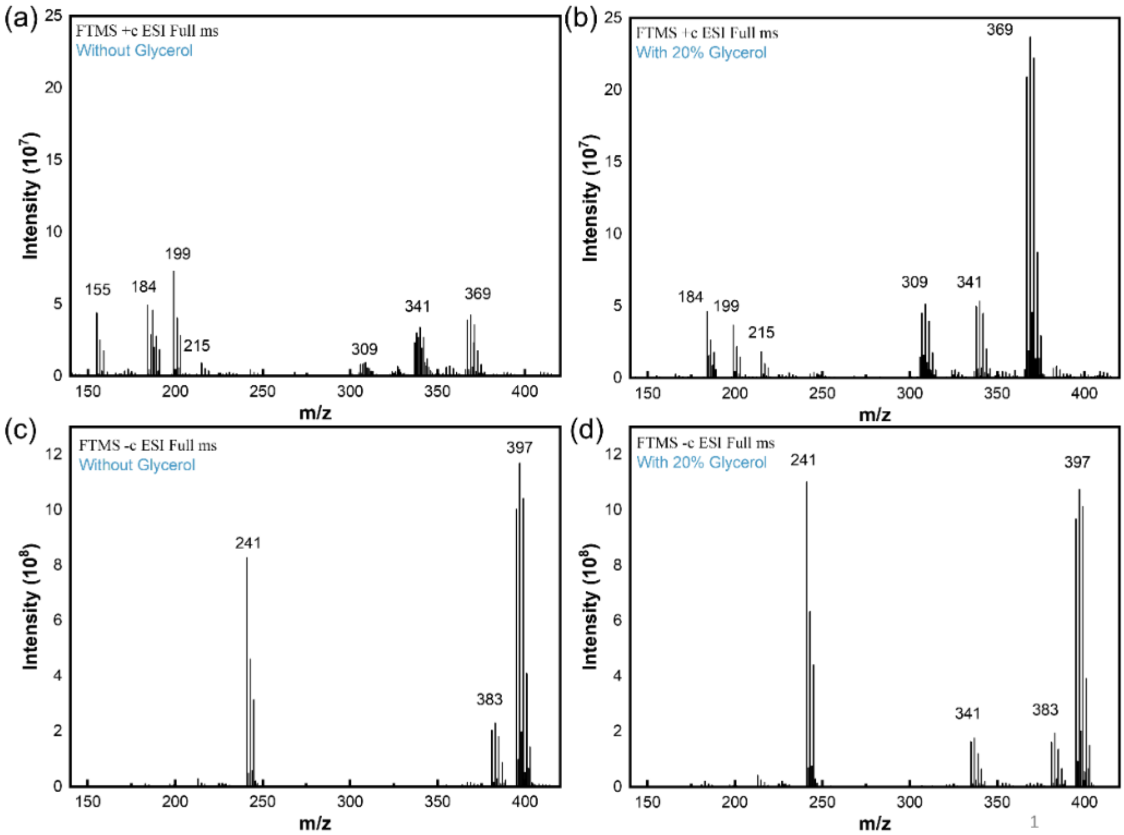

Figure S10. The results of liquid chromatography–mass spectrometry of the precursor solution with or without glycerol. (a) and (b) are the analysis result by the cation mode. (c) and (d) are the analysis result by the anion mode.

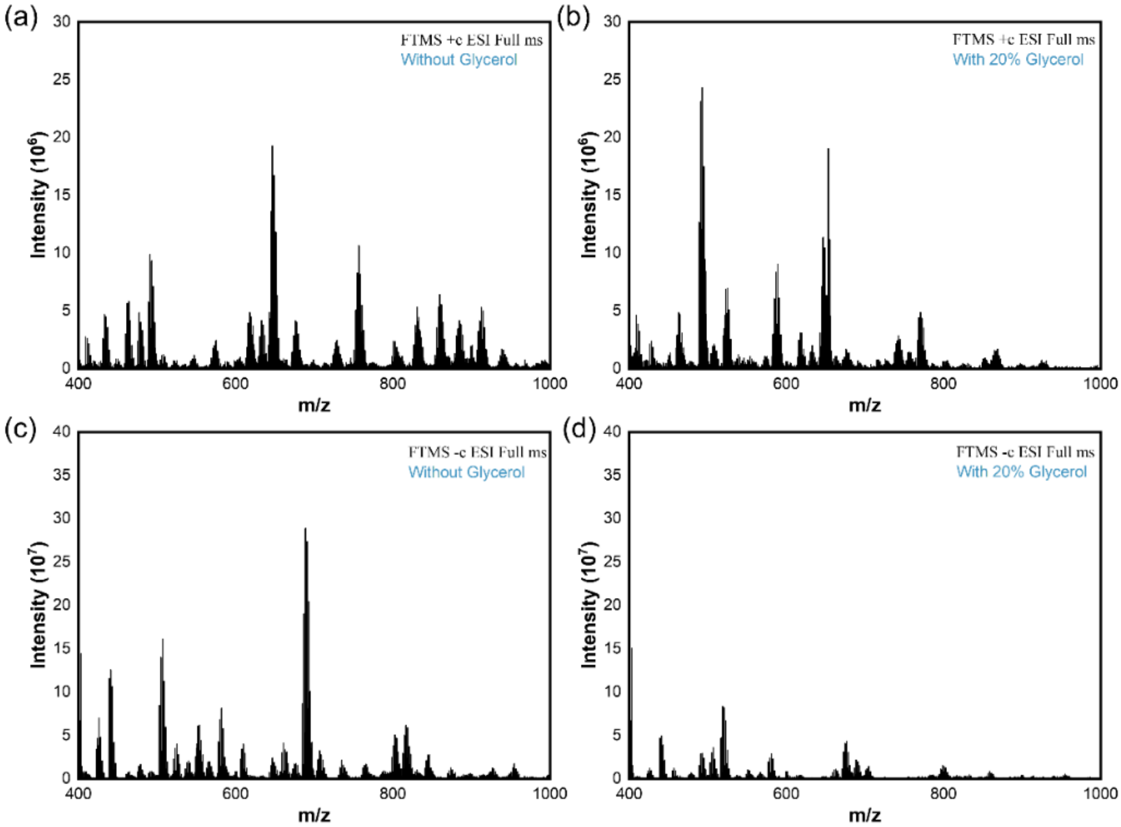

Figure S11. The results of liquid chromatography-mass spectrometry of the molecules with a mass-to-charge ratio greater than 400. (a) and (b) are the analysis results of the cation mode. (c) and (d) are the analysis results by the anion mode.

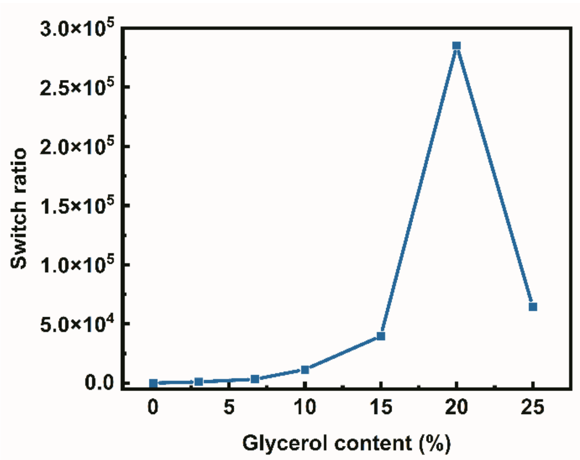

Figure S12. The switching ratio of ZnO UV detector with varying glycerol concentrations

Supporting Table:

Table S1 Summary the photoresponse of UV photodetectors based on ZnO materials

Material	On/Off ratio/ light power intensity	Responsivity (A/W)	I_{dark} (A)/ Bias voltage	Fabrication Method	Ref.
rGO/ZnO	~2 (20.03 mW/cm^2)	3.24	3.9×10^{-6} /1V	Selective FsLDW	1
ZnO NRs	7.5×10^5 (20 mW/cm^2)	2.81	3.5×10^{-9} /10V	Wet screen printing	2
ZnO NWs	300 (0.43 mW/cm^2)	4×10^4	10^{-8}~10^{-9}/5V	Fs laser 3D assembly	3
ZnO NWs	250 (2.5 μW/cm^2)	2×10^7	~10^{-8}/1.5V	Contact printing	4
ZnO/PEG	2.8×10^5 (10.15 mW/cm^2)	1.77	2.57×10^{-10}/3V	Drop casting	5
ZnO NWs	2.5×10^3 (2 μW/cm^2)	55	10^{-9}/5V	spray coating	6
ZnO granular NWs	~10^6 (77.5 μW/cm^2)	7.5×10^6	2×10^{-11}/1V	Near-field electrospinning	7
Patterned ZnO NPs	2.8×10^5 (2 mW/cm^2)	2.78×10^2	<10^{-11} /10V	Glycerin-assisted FsLDW	Our Work

References

1. An, J. et al. Single-Step Selective Laser Writing of Flexible Photodetectors for Wearable Optoelectronics. *Advanced Science* **5**, 1800496 (2018).

2. Qu, M. et al. Dry-Wet Hybrid Direct Printing of Laser-Induced Graphene and Zinc Oxide Nanoribbons for Continuous-Flow Manufacturing of Flexible Wearable Photodetectors. *Advanced Materials Technologies* **9**, 2302056 (2024).

3. Long, J. et al. Directional Assembly of ZnO Nanowires via Three-Dimensional Laser Direct Writing. *Nano Letters* **20**, 5159-5166 (2020).

4. Christou, A. et al. Printing of Nano- to Chip-Scale Structures for Flexible Hybrid Electronics. *Advanced Electronic Materials* **9**, 2201116 (2023).

5. Yang, D. et al. Sunscreen-Inspired ZnO/PEG Composites for Flexible Ultraviolet Photodetectors with a Giant On–Off Ratio. *ACS Photonics* **10**, 1320-1327 (2023).

6. Yalagala, B.P., Dahiya, A.S. & Dahiya, R. ZnO nanowires based degradable high-performance photodetectors for eco-friendly green electronics. *Opto-Electronic Advances* **6**, 220020 (2023).

7. Liu, X. et al. All-printable band-edge modulated ZnO nanowire photodetectors with ultra-high detectivity. *Nature Communications* **5**, 4007 (2014).